10

Fetal Cardiac Magnetic Resonance (CMR)

Sahar N. Saleem
Radiology Department-Faculty of Medicine Kasr Al-Ainy-Cairo University
Egypt

1. Introduction

Congenital heart disease (CHD) is present in 0.8% of all live births and is therefore one of the most common congenital malformations (Fyler et al., 1980). The spectrum of congenital heart defects is significantly higher in fetuses than in live born infants because of their reduced viability (Tennstedt et al., 1999). The prognosis of congenital heart disease can be poor; almost one third to one half of congenital heart defects are severe and lethal unless an intervention is done early (Hoffman & Kaplan, 2002). Prenatal diagnosis of congenital heart disease results in referral of mothers with affe1cted fetuses to equipped centers where all facilities for neonatal cardiac care are available. The diagnosis of a congenital heart disease in a fetus should also prompt evaluation for genetic syndromes and associated non cardiac malformations (Cohen, 2001). Improvements in diagnosis and treatment have lead to more patients surviving to adulthood (Carvalho et al., 2002).

Echocardiography is the gold standard diagnostic imaging tool for prenatal detection of cardiac malformations (Kleinman et al., 1980). Fetal echocardiography combines the benefit of accurate assessment of cardiac anatomy and function probability (Carvalho et al., 2002). However, Ultrasonography (US) is occasionally limited by acoustic window, poor images of the distal vasculature, fetal position, maternal adipose tissue, abdominal wall scar form previous abdominal or pelvic surgery, and is user dependent (Forbus et al., 2004). As a consequence, there remains room for other modalities in studying the fetal cardiovascular system.

Cardiac Magnetic Resonance imaging (CMR) proved unequivocal advantages over other cardiac imaging modalities (Prakash et al., 2010). Technical advances during the last decade have brought CMR into the mainstream of noninvasive cardiac imaging. The clinical applications of CMR are well-established in pediatrics and adults patients. CMR is employed in clinical practice of congenital heart disease, cardiac masses, the pericardium, right ventricular dysplasia, and hibernating myocardium. Role of CMR includes anatomic and functional assessment of the cardiovascular system (Finn et al., 2006). Fetal MRI proved valuable in defining the details of fetal anatomy especially the central nervous system (Frates et al., 2004; Levine, 2006; Saleem et al., 2009) and potentially the heart (Gorincour et al., 2007; Saleem, 2008). However, CMR has not been thoroughly investigated in-utero.

2. Fetal Cardiac Magnetic Resonance (CMR)

The intent of this chapter is to serve as a primer for fetal Cardiac Magnetic Resonance (CMR) based on our clinical cases of normal and abnormal fetal hearts. The chapter will

include discussion of fetal Magnetic Resonance Imaging (MRI); fetal CMR technical aspects; MRI anatomy of the fetal heart; in-utero diagnosis of CHD and associated fetal syndromes; and future of fetal CMR.

2.1 Fetal Magnetic Resonance Imaging (MRI)

2.1.1 Fetal MRI: Safety and ethics

Magnetic Resonance Imaging (MRI) is a non-invasive diagnostic examination that does not involve ionizing radiation with no known associated negative side effects or delayed sequels to date (Clements, 2000). However, because of the potential risk of MR imaging to the developing fetus it is always prudent to follow MR imaging ethics. The American College of Radiology (ACR) white paper on MR safety states that Fetal MR imaging is indicated if the risk-benefit ratio to the patient warrants that the study be performed (Kanal et al, 2002). According to The Safety Committee of the Society of MRI, fetal MRI is only indicated if other non-ionising diagnostic imaging methods are inadequate. It is also prudent to wait until after the first trimester before performing fetal MRI. (Glenn & Barkovich, 2006).

2.1.2 Fetal MRI: General indications

Fetal MRI is indicated to evaluate abnormalities and underlying etiologies that are not as readily depicted with Ultrasonography (US). In contradistinction to US, MRI visualization of the fetus is not significantly limited by maternal obesity, fetal position, or oligohydramnios and visualization of the brain is not restricted by the ossified skull (Levine, 2006). MRI provides superior soft tissue contrast resolution and the ability to distinguish individual structures such as brain, lung, liver, kidney, and bowel. MRI provides multiplanar imaging as well as a large field of view, facilitating examination of fetuses with large or complex anomalies, and visualization of the lesion within the context of the entire body of the fetus (Frates et al, 2004).

2.1.3 Fetal MRI: Technical aspects

MRI is performed on 1.5 T superconducting magnet and a phased-array surface coil. The mother lies supine during the examination. If the mother does not tolerate the supine position, MRI should be performed in the left lateral decubitus. No special preparations, fasting, or sedation are required (Levine, 2006).

Initial attempts at MRI of the fetus were challenging because of fetal motion and altered fetal position which produced significant imaging artefacts. Development of fast MRI sequences significantly decreased motion artifacts and eliminated the need for fetal sedation (Levine, 2006).

A variety of fast MRI sequences are currently available including single-shot fast spin echo (SSFSE) or half Fourier acquired single shot turbo spin echo (HASTE) to obtain T2-weighted images, fast gradient echo sequences with low flip angle shot (FLASH) to obtain T1-weighted images, and steady state free precession sequence (balanced fast field echo b-FFE) to obtain a balanced image (Brugger et al, 20006; Chung et al, 2000).

In young fetuses (less than 16 weeks' gestation) fetal movements will reduce the conspicuity of fetal anatomy. Small structures are especially difficult to identify early in gestation. With advancing gestation, the reduced fetal motion and the increased size of fetal structures will progressively enhance anatomical visualization (Frates et al, 2004). In addition, the general limitations of fetal MRI include the high costs, the limited availability, in addition to MRI-specific absolute contraindications like maternal pacemakers and ferromagnetic implants. Claustrophobia can be an additional issue, especially as pregnant women can have difficulties lying on their back, mainly in the third trimester (Saleem et al, 2009).

2.2 In-utero MR imaging of the fetal heart

2.2.1 Feasibility and patients' selection

MRI of the fetal heart is feasible (Saleem, 2008); however, it has not been thoroughly investigated with only few reports in literature most of them in the form of case reports or preliminary experiences (Gorincour et al, 2007; Kivelitz et al, 2004; Manganaro et al, 2008). We will depend in discussion of MRI of fetal heart in this chapter on findings from our study of 298 pregnancies at high risk for CHD that were enrolled sequentially from September 2003 to August 2010 in our institutional review board-approved study. The mean gestational age was 24 weeks with a range of 16-36 weeks.

Patients were eligible for enrolment if they were at possible risk for CHD or for an abnormality detected in fetal echocardiography. Risk factors for CHD were combination of history of previous pregnancies with CHD, a parent with CHD, maternal Rubella infection, maternal collagen disease, maternal Diabetes Mellitus, maternal exposure to a possible teratogen (Phenytoin medication), or abnormal findings in prenatal echocardiography. Written informed consent was obtained from all of the expectant mothers before MRI.

2.2.2 Technique

MRI was performed with a 1.5-T superconducting magnet (Gyroscan Intera, Philips Healthcare) and a phased-array surface coil. No maternal sedation, fetal sedation or paralysis, fetal cardiac gating, or controlled maternal breathing was used. The imaging time for the examination ranged between 15-45 minutes (20 minutes in average).

MR sequences include (Fig. 1):

a. **Bright blood sequences** using balanced steady-state-free-precession sequences (balanced-SSFP). Balanced SSFP sequences (Repetition time TR/Echo time TE, 3.5–4/1.7–2; flip angle FA, 60–90°; slice thickness, 3–5 mm; gap, 1 mm to section overlap of –3 mm) were performed for all patients. The thin overcontiguous sections are used for evaluation of small fetuses. The field of view FOV (205–350 mm2) is adjusted to increase or decrease in the fetal or maternal dimensions or when aliasing artifact is a problem. The matrix size is 183 x 256 or 256 x 256 according to the selected FOV; reduction of FOV compelled reduction of matrix size in some cases. One to three signals are averaged. The imaging time for each sequence depends on the number of slices and number of signals averaged.

b. **Dark blood sequences** using T2-weighted single-shot fast spin echo sequences (TR/TE 1000/151, Matrix 256 × 134, slice thickness 3 mm, FOV (205–350 mm2).
c. **Additional T1** Fast gradient echo sequence with low Flip angle shot was: TR/TE of 100-140/4.2 ms, 70-90° FA, 256x160-256 matrix, one signal acquired, slice thickness 4-6 mm with an inter-slice gap of 0.2-0.4 mm.

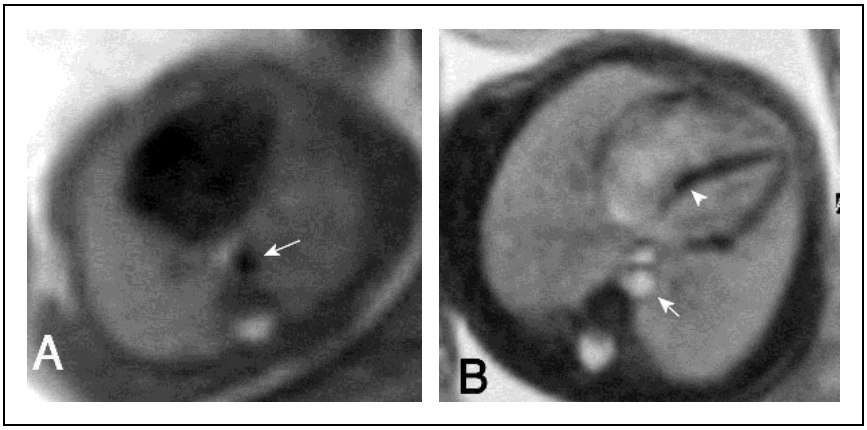

Fig. 1. Axial MR images of fetal thorax at 24 weeks' gestation using dark blood sequence single shot fast spin echo (SSFSE) (A) and bright blood sequence steady state free precession (SSFP) (B). SSFP is superior in visualizing cardiac morphology, interventricular septum (arrowhead) and thoracic aorta (arrows).

Planes:

A scout acquisition is performed (single shot fast spin echo: TR/TE 10000/100 msec, 4 mm slice thickness, matrix 196x256x256) is taken on maternal coronal or axial planes to determine fetal position for situs assessment. Series of images are then taken along the three fetal body planes and cardiac planes using mainly balanced SSFP (Fig. 2).

a. **Fetal body planes:** A series of images are taken along the three fetal body planes (axial, sagittal, and coronal). Each new acquisition is prescribed by use of images from the immediately previous acquisition to avoid misregistration caused by fetal movement. Additional images are obtained along the planes of the brain and any other suspected extra-cardiac region.
b. **Cardiac axes:** MR imaging are also attempted along cardiac axes. A representative image from each sequence is used as a scout to align the subsequent acquisition. From the coronal plane, the long-axis view is obtained along a line that extended from the cardiac apex to the middle of the left ventricle. A short-axis view perpendicular to the long axis also is obtained. In the short-axis view, the image in which the left ventricle is concentric and the right ventricle is crescent-shaped is chosen to align the plane for the four-chamber view. The plane for the four-chamber view extends along the center of the left ventricle and the farthest corner of the right ventricle. From the four-chamber image, the two-chamber view is obtained along the right and left sides of the heart (Saleem, 2008).

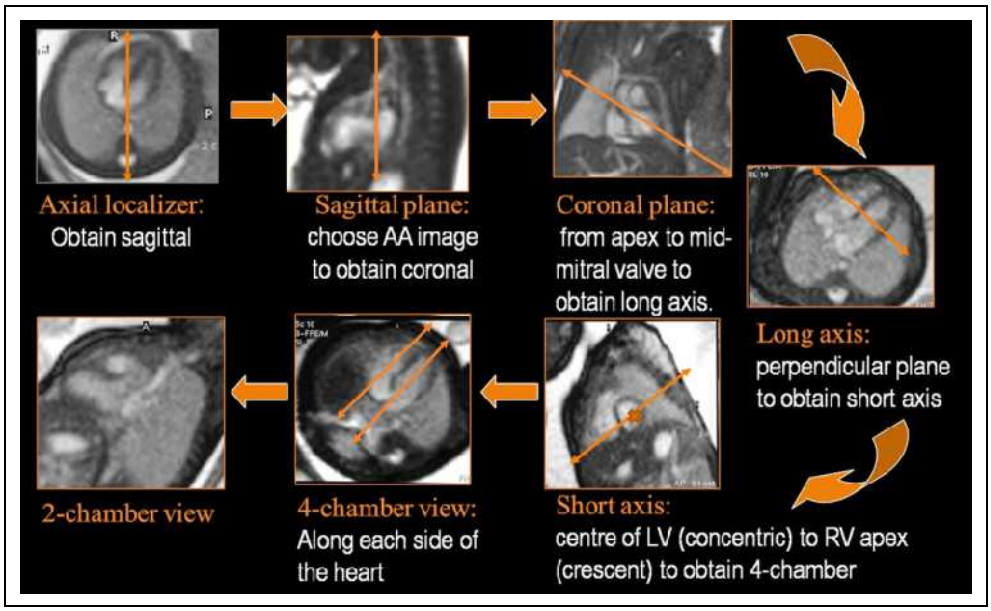

Fig. 2. MR imaging of fetal heart along three fetal body planes as well as cardiac axes.

2.2.3 MRI anatomy of the fetal heart

MRI anatomy of fetal heart in Axial plane: The figure (Fig.3) shows axial MR images (upper row) of a fetal heart in comparison to equivalent echocardiographic views (lower row) arranged from caudad to cephalad. At the level of the four cardiac chambers (Fig. 3A), the interventricular septum is central, cardiac axis is 45 degrees; both atria and both ventricles have comparable size. Atrio-ventricular and great arteries valves are occasionally seen. At a superior level (Fig. 3B), the left ventricular outflow tract (LVOT) can be seen. At the level of the right ventricular outflow tract (Fig. 3C), images show bifurcation of the main pulmonary artery to right and left pulmonary arteries. MR image can show the main bronchi in relation to the pulmonary artery branch which helps in assessment of the viscero-atrial situs; tracheobronchial tree cannot be seen on echocardiography. The three-vessel-view (Fig.3D) shows the aorta winds around the trachea as well as the left brachiocephalic vein which meets the right to form superior vena cava (SVC).

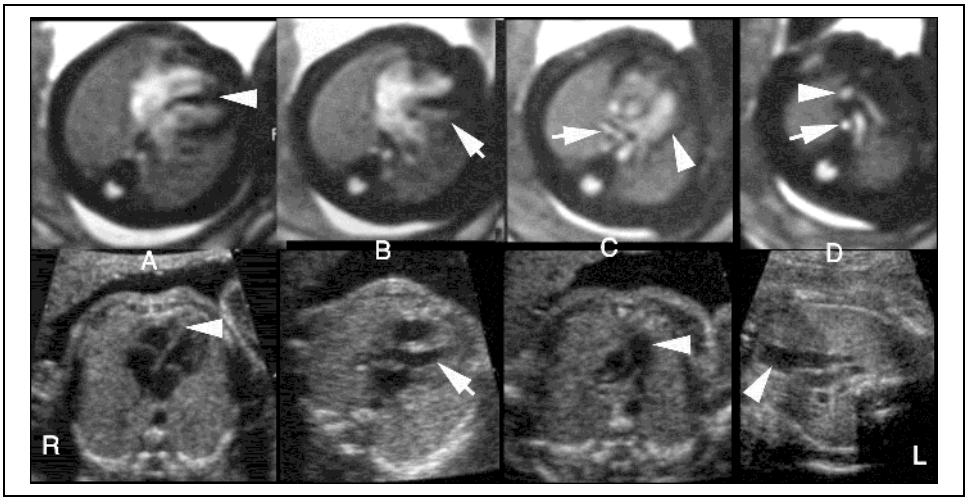

Fig. 3. Comparable axial anatomy of the fetal heart (at 26 weeks' gestation) in MRI (upper row) and echocardiography (lower row) from caudad to cephalad; R: right, L: left. (A) Four-cardiac-chamber view: arrowheads point to interventricular septum. (B) Left ventricular outflow tract (LVOT) view: arrows point to (LOVT). (C) Right ventricular outflow tract (RVOT) view: arrowheads point to the bifurcating main pulmonary artery; arrow in upper MR image points to the right main bronchus posterior to the right pulmonary artery. (D) Three-vessel-view: arrowheads point to the right brachiocephalic vein which meets its left counterpart to form superior vena cava (SVC). Aorta winds around the trachea (arrow in upper MR image points to fluid-filled trachea).

MRI anatomy of fetal heart in Coronal plane: In this plane, MRI shows cardiac apex, left ventricle, LVOT, inflow systemic veins and their tributaries drain to the right atrium, brachiocephalic veins join to form SVC, and hepatic veins drain to inferior vena cava (IVC) (Fig. 4).

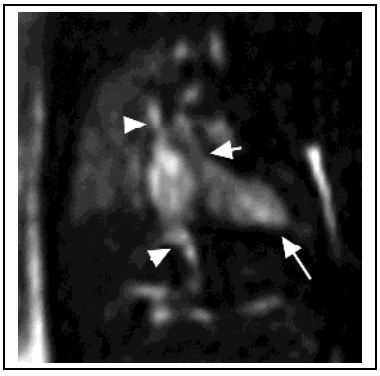

Fig. 4. Coronal MRI of normal fetal heart at 24 weeks' gestation shows SVC and IVC (arrowheads) draining into right atrium, cardiac apex (long arrow), and LVOT (short arrow)

MRI anatomy of fetal heart in sagittal plane: MRI shows in sagittal plane (Fig. 5) systemic inflow veins and connection between right ventricle and its outflow tract.

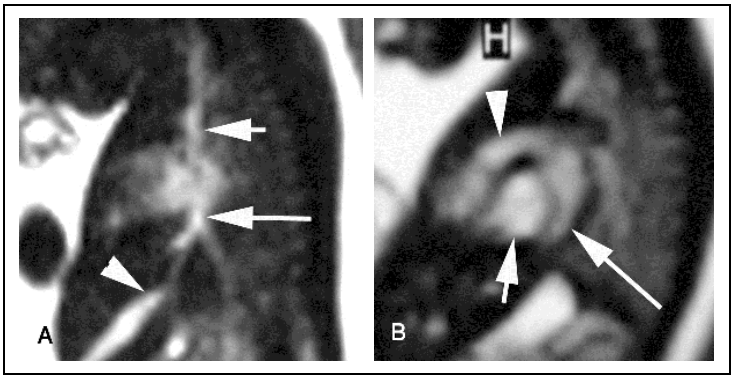

Fig. 5. Sagittal anatomy of normal fetal heart at 24 weeks' gestation obtained from right to left direction. (A) The image shows superior (short arrow) and inferior (long arrow) venae cave draining to right atrium. Umbilical vein (arrowhead) is also seen draining into IVC. (B) The image shows the pulmonary artery (arrowhead) originating from the right ventricle. Short arrow points to the left ventricle, and long arrow points to the left atrium.

MRI anatomy of fetal heart along cardiac axes (Fig.6 & Fig. 7). MR imaging along different cardiac axes reveals details of the fetal cardiac structures. Imaging along the long cardiac axis (Fig. 6A) and four cardiac chamber view (Fig. 6B) can show detailed morphologic features of the cardiac chambers namely the moderator band, atrial septal duct valve, foramen ovale, and pulmonary veins.

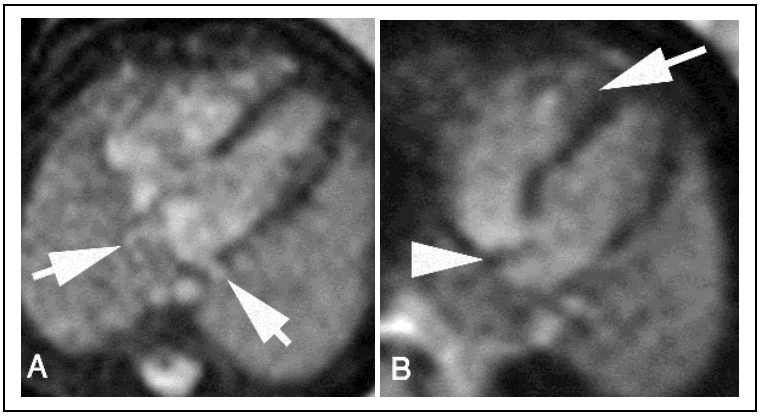

Fig. 6. MRI anatomy of fetal heart at 28 weeks' gestation along long cardiac axis (A) and 4-chamber view (B). In (A), arrows point to pulmonary veins. In (B), moderator band (arrow) appears as low signal intensity structure between the apical right ventricular septum and free right ventricular wall. Atrial septal duct valve (arrowhead) is directed to the left indicating the normal blood direction across the foramen ovale in fetal life from right to left

MR imaging along the short axis plane (Fig.7A) and two-cardiac-chamber view (Fig. 7B) of the fetal heart can show well the connection between the ventricles and great vessels.

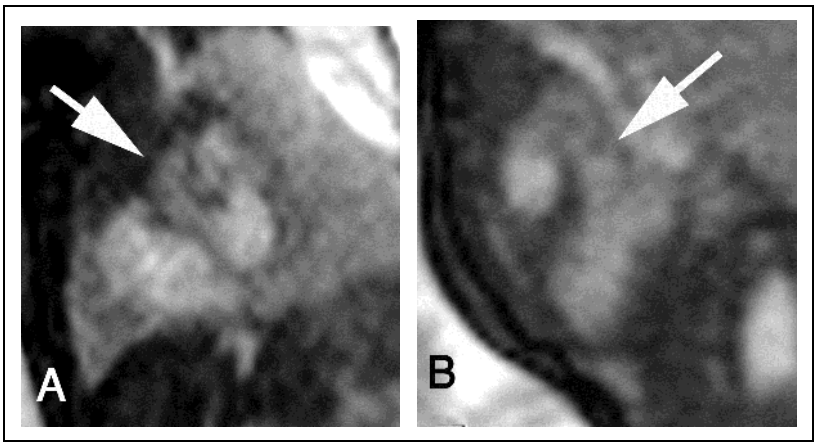

Fig. 7. MRI anatomy of fetal heart at 28 weeks' gestation displayed in short cardiac axis (A) and two-cardiac chamber view along the left heart (B) using b-SSFP sequence. Arrows in both views point to left ventricular outflow tract originating from the left ventricle

2.2.4 Image interpretation of fetal CMR

Prenatal echocardiographic images are analyzed with anatomic segmental approach to congenital heart disease (Carvalho et al, 2005). A modified segmental approach can be used to analyze MR images of the fetal heart (Saleem, 2008) that includes the following:

Visceroatrial situs: The stomach is normally on the left side, IVC on the right side, the embryologic left bronchus is long with no early division and runs under the left pulmonary artery, and the right bronchus is short and runs behind the right pulmonary artery.

Cardiac position: Most of the heart occupies normally the left side of the thorax with the cardiac apex to the left.

Cardiac size: The heart occupies normally one third of the thorax.

Cardiac axis: The cardiac axis is the angle between the true sagittal plane (between the spine and the anterior chest wall) and a plane along the interventricular septum.

Cardiac chambers: The cardiac chambers are evaluated for number (normally four), arrangement (left atrium normally is close to the fetal spine), relative size of both atria (normally equal in size), and relative size of both ventricles (normally equal in size). Moderator band identifies the morphological right ventricle. Foramen ovale and atrial septal duct valve location (presence in the left atrium indicates normal right-to-left blood flow). Intactness of interventricular septum and appearance of valves (atrioventricular and great arterial).

Ventricular looping: In a normal D-loop, the more anterior ventricle is the embryologic right one.

Inflow veins: Superior and inferior venae cavae normally connect to the right atrium. Two right and two left pulmonary veins normally join the left atrium; at least one pulmonary vein can be visualized in fetal CMR.

Outflow vessels: The left and right ventricular outflow tracts (aorta and pulmonary arteries) are evaluated for relative size (normally equal) and relative position in relation to each other (normally cross perpendicular in relation to their origin).

Ventriculoarterial concordance: Normally the aorta arises from the left ventricle. It can be traced in a regular arch that gives rise to three neck vessels. The pulmonary artery normally arises from a morphologic right ventricle and bifurcates at its distal end.

Side of the aortic arch: The side of the aortic arch is defined according to the main bronchus, above which it crossed the mediastinum posteriorly (Saleem, 2008).

2.3 Abnormal findings in fetal CMR

We include abnormal fetal cardiac findings detected upon using a modified segmental approach in analysis of CMR from our series of 298 pregnancies.

Viscero-atrial situs

MR imaging along maternal coronal or axial planes enables determination of fetal position for situs assessment. In situs inversus totalis, cardiac apex and stomach are detected on the right of the fetal body on coronal MR images (Fig. 8A). In heterotaxy, fetal CMR can detect a combination of cardiac, vascular and visceral abnormalities. In left atrial isomerism where left-sided organs are paired and right-sided structures may be absent, fetal MRI detected dextrocardia, central liver, polysplenia, and interrupted inferior vena cava with azygous continuation (double vessel sign) (Fig. 8B).

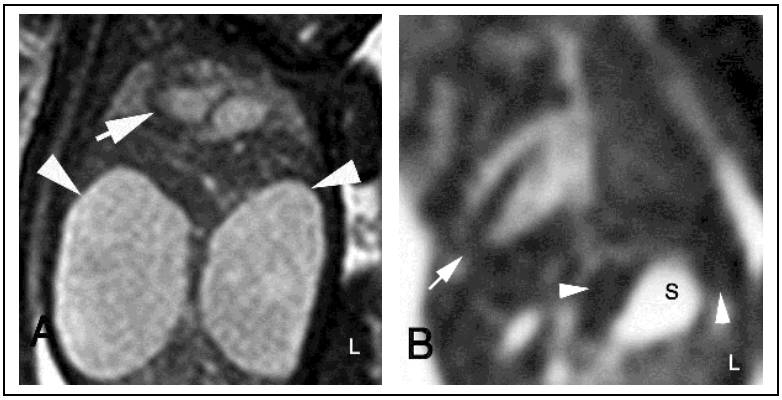

Fig. 8. Viscero-atrial situs abnormalities can be detected in fetal CMR in coronal (T2-SSFP) image. (A) In a 27 weeks' gestation fetus with situs inversus totalis, arrow points to right-sided cardiac apex and arrowheads point to associated hepatic cysts. (B) In a 20 weeks' gestation fetus with left atrial isomerism the cardiac apex points to the right (dextrocardia) (arrow). The fluid-filled stomach (s) occupies the left upper abdomen and is surrounded by multiple widely-spaced masses with low signal intensity characteristic for polysplenia

Cardiac Position and axis

In four-chamber transverse MRI view, most of the fetal heart normally occupies the left side of the thorax with the cardiac apex to the left. In a previous study of normal fetal hearts using MRI, the cardiac axis measurement (37.25° ± 7.15°) (Saleem, 2008) was in comparable with sonographic norms of (43° ± 2°) (Smith et al, 1995). When the axis of the heart is not within the normal range, the fetus is at increased risk of heart malformation or abnormal intrathoracic anatomy (Cohen, 2001). MRI axial four-chamber view depicts the fetal cardiac position and enables measurement of cardiac axis. Placement of the heart outside the chest (ectopia cordis) is a rare extreme cardiac position abnormality (Fig.9).

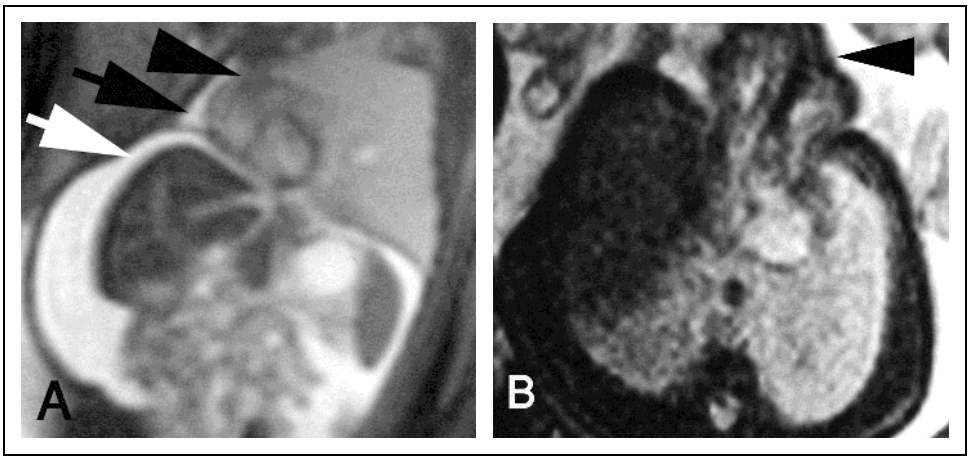

Fig. 9. Cardiac position abnormalities detected in fetal CMR. (A): Coronal T2-weighted SSFP image of a torso of 27 weeks' gestation fetus with cardiac position abnormality due to intrathoracic lesion. Arrowhead points to a deviated heart to the right hemithorax caused by intrathoracic abnormalities (hypoplastic right lung). Black arrow points to right pleural effusion and white arrow to associated ascites. (B): Axial T2-weighted SSFP of chest of 28 weeks' gestation fetus with ectopia cordis as part of Pentalogy of Cantrell. The axial image shows well the herniating heart (arrowhead) through the defective anterior chest wall

Balanced cardiac chambers

Four-cardiac-chamber and long-axis-cardiac MR views are valuable in assessing the number of chambers (normally four) of fetal heart as well as in comparing the sizes of both atria and both ventricles (normally have comparable sizes).

Detection of a balanced four-cardiac chamber view allows exclusion of odd number of chambers and unbalanced abnormalities of atrioventricular valves such as atresia (Saleem, 2008). In our experience, CMR allowed detection of imbalanced cardiac chambers in-utero (Fig.10). Abnormal decrease in size of cardiac chambers was detected by fetal CMR in cases such as hypoplastic left heart and hypoplastic right heart. In our series, fetal CMR also depicted abnormal increase in the size of individual fetal cardiac chamber such as dilatation of right atrium in Ebstein's anomaly and dilated right atrium in fetuses with partial anomalous pulmonary venous drainage.

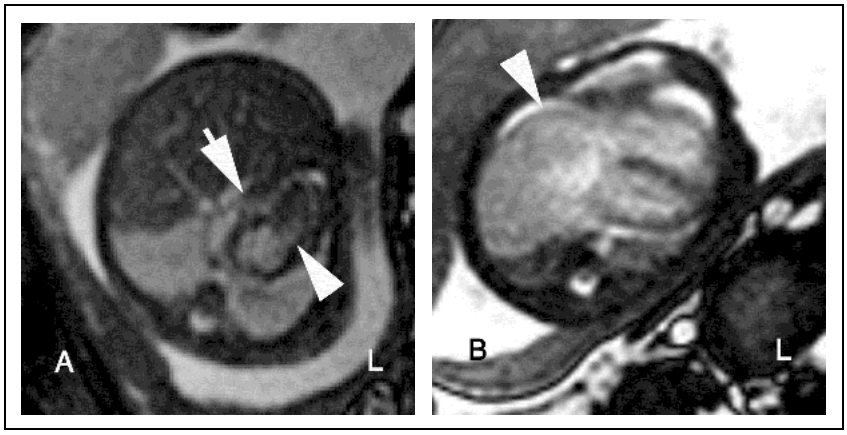

Fig. 10. Imbalanced fetal cardiac chambers detected four-chamber T2- SSFP CMR image. (A): A 24 weeks' gestation fetus with hypoplastic right heart (arrow) shows discrepancy in size with the normal left heart (arrowhead). (B) A 28 weeks' gestation fetus with Ebstein's anomaly shows aneurismal dilatation of the right atrium (arrowhead).

Intactness of interventricular septum: Interventricular septum appears in T2-SSFP fetal MR images as thin low signal intensity structure that separates the right and left ventricles (Fig.1B). Transverse four-chamber and long axis MR images are valuable in assessment of interventricular septum of fetal heart. Defects in the interventricular septum can be detected in fetal CMR as an isolated cardiac abnormality or part of a more complex heart anomaly (Fig.11).

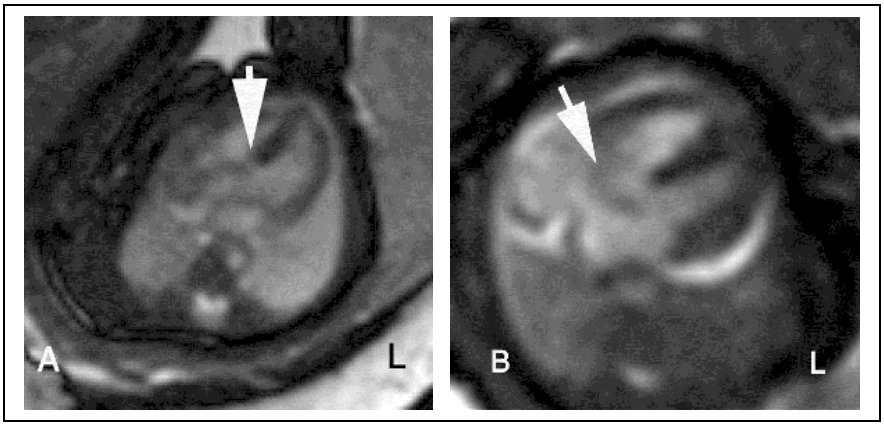

Fig. 11. Interventricular septal defects are detected in four-chamber T2-SSFP fetal CMR. (A) In a 25 weeks' gestation fetus with Trisomy 13, MR image shows a small high interventricular septal defect (VSD). (B). In a 30 weeks' gestation fetus, MR image shows a large atrioventricular septal defect (AV canal) (arrow) as part of a complex cardiac anomaly in association with transposition of great arteries (TGA) (not shown).

Inflow vessels: Superior and inferior venae cavae (SVC, IVC) can be detected draining to right atrium on coronal and sagittal fetal CMR. Normally, at least one pulmonary vein can be visualized in 4-chamber view draining to the left atrium (Saleem, 2008). Fetal CMR can diagnose inflow vessels abnormalities such as persistent left SVC (Fig.12) as well as anomalous pulmonary venous drainage.

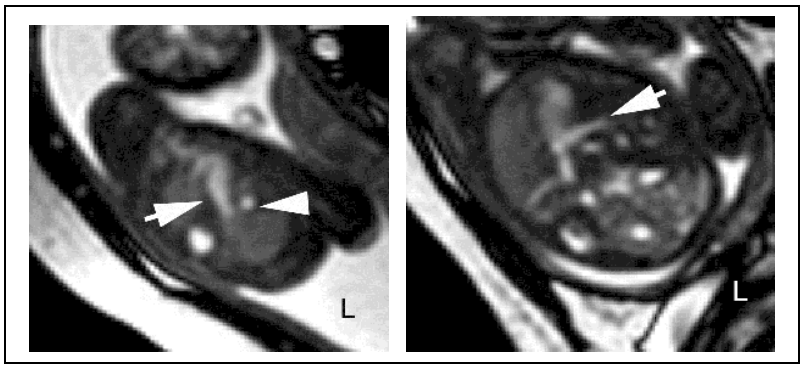

Fig. 12. Left superior vena cava (SVC) diagnosed by axial T2- SSFP MRI at 26 weeks' gestation. (A) Three-vessel axial image documents absent right and persistent left SVC (arrowhead) as well as right sided aortic arch (arrow). (B) Axial MR image caudad to (A) shows left SVC (arrow) draining into a dilated right coronary sinus.

Outflow vessels: In fetal CMR, left ventricular outflow tract (Aorta) can be detected on axial, coronal, and short axis views. Right ventricular outflow (pulmonary artery) tract can be identified on axial, sagittal and short axis views. Outflow vessels are normally equal in size and cross at their origin. Fetal CMR can detect conotruncal abnormalities (Fig. 13) such as transposition of great arteries (TGA), truncus arteriosus, Fallot's, and coarctation of aorta.

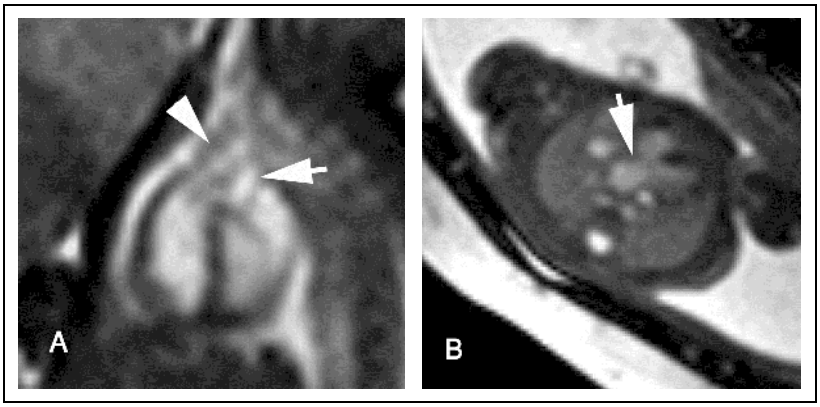

Fig. 13. T2-SSFP CMR diagnoses outflow vessels abnormalities in-utero. (A) Sagittal MRI of 30 weeks' gestation fetus with TGA shows parallel course of Pulmonary artery (arrowhead) and aorta (arrow) at their origin (Same fetus in Fig.11A). (B) Axial MRI of 26 weeks' gestation fetus shows a single outflow tract (truncus arteriosus) (arrow) over-rides VSD

Ventriculoarterial concordance: Fetal CMR using T2-SSFP can identify the morphological right ventricle through identification of the moderator band (Fig. 6B). The pulmonary artery normally arises from a morphologic right ventricle and bifurcates at its distal end. While the aorta arises from the left ventricle and can be traced in a regular arch that gives rise to three neck vessels.

Side of the aortic arch: The side of the aortic arch is defined according to the main bronchus, above which it crossed the mediastinum posteriorly (Saleem, 2008). The aortic arch is usually on the left. Right sided aortic arch can be detected on fetal CMR as an isolated finding or part of a complex cardiac malformation (Fig. 12A).

Cardiac masses and pericardial fluid: primary cardiac tumors are rarely diagnosed in utero and are usually seen on prenatal echocardiography. Few cases of cardiac rhabdomyomas have been reported in-utero by MRI (Kivelitz et al, 2004). On T2-SSFP sequence, fetal cardiac rhabdomyomas appear as low signal intensity masses in contrast with the high signal intracardiac blood. On T2-SSFSE, cardiac rhabdomyomas are less conspicuous as they appear of intermediate signal intensity against the low signal intensity intracardiac blood. Fetal CMR enabled precise detection of size and location of cardiac rhabdomyomas in multiple planes as early as 16 weeks' gestation (Fig. 14). Fetal CMR can identify well pericardial effusion as an isolated finding or in association with structural cardiac anomalies or hydropes fetalis (Fig. 14B).

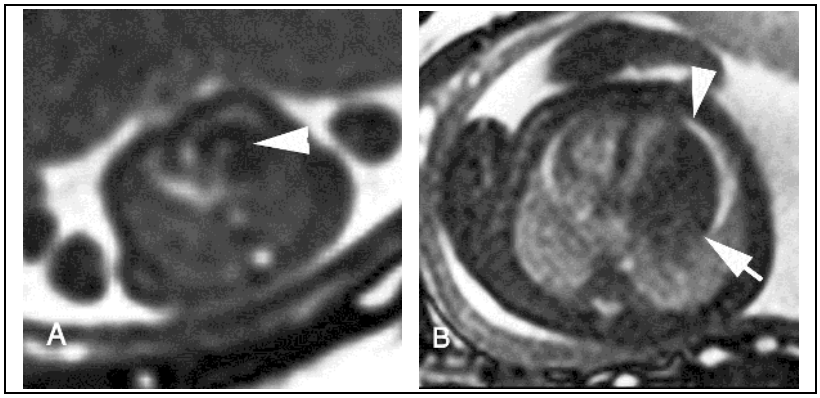

Fig. 14. In-utero MR imaging of cardiac rhabdomyomas. (A) Axial T2-SSFP four-chamber view of 16 weeks' gestation fetus show low signal intensity rhabdomyoma of the free left ventricular wall and interventricular septum (arrowhead). (B) Axial T2- SSFP four-chamber view of 26 weeks' gestation fetus shows a large intracardiac mass (rhabdomyoma) within the left ventricle (arrow). Note the associated high signal intensity rim of pericardial effusion (arrowhead).

2.4 Fetal CMR findings in complex congenital heart disease (CHD), CHD associated with extra-cardiac abnormalities and fetal syndromes

Multiple cardiac abnormalities can be concomitant in complex congenital heart diseases (Cohen et al, 2001). In our experience, in-utero MRI using SSFP sequence was useful in assessment of fetal heart anatomy and depiction of multiple cardiac structural abnormalities in complex congenital heart diseases in CHD. E.g., in Fallot's disease, fetal CMR identified

septal defects (ventricular septal defect (VSD) in Fallot's tetralogy and atrioventricular (AV) canal in Fallot's pentalogy respectively) in association with overriding of aorta and stenotic pulmonary artery. CMR diagnosed a fetus with Transposition of great arteries (TGA) (Fig.13A) in concomitant with AV canal.

Complex congenital cardiac anomalies can be seen in the rare conjoined heart twins. Conjoined twins result from a separation defect in the embryonic plaque between the 13th and 17th days of gestation. Cardiac fusion is a very rare malformation that can be seen in twins conjoined at the level of the chest (Thoracopagus). Detailed evaluation of the degree of union and number of shared organs is required to predict the viability and prognosis of fetuses (O'Neill et al, 1988). In our series, fetal CMR helped in conjunction with ultrasonography in prenatal assessment of a thoracopagus conjoined twins with a shared eight-chamber heart and in a dicephalic twin with a shared 4-chamber heart (Fig. 15).

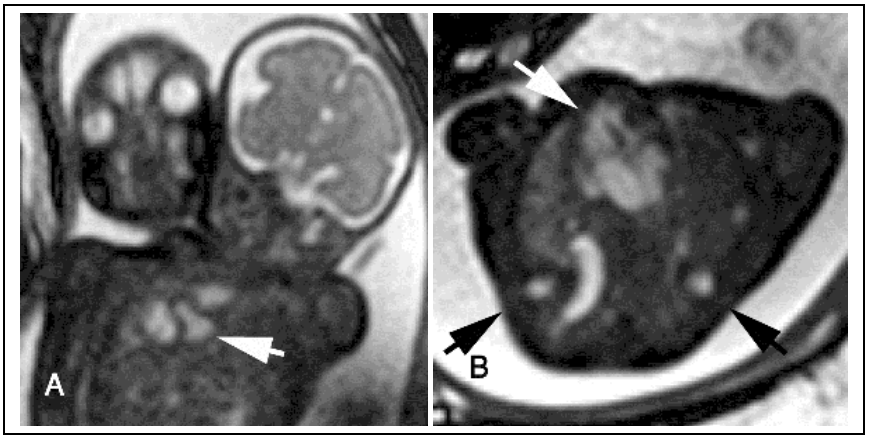

Fig. 15. In-utero CMR of dicephalic twin with a shared 4-chamber heart (A) Coronal T2-SSFP identifies dicephalic tripus dibrachius twin with single heart (arrow). (B). Axial T2-SSFP shows double spine (black arrows) and a single four chamber heart (white arrow).

Complex cardiac anomalies are frequently associated with extra-cardiac malformations (Prakash et al, 2010). The diagnosis of a congenital heart disease in a fetus should include prompt evaluation for associated non cardiac malformations and diagnosis of genetic syndromes (Carvalho et al, 2002). In-utero MRI can depict extracardiac anatomy and abnormalities of fetal brain, spine, lungs, liver, spleen, kidneys, and gastro-intestinal tract (Frates et al, 2004; Levine, 2006, Saleem et al, 2009). In our series, fetal MRI detected extracardiac abnormalities in association with cardiac structural abnormalities that helped in prenatal diagnosis of fetal syndromes. Extracardiac abnormalities associated with CHD include central nervous system, cranio-facial, urinary tract, lungs, gastrointestinal tract, liver, spleen, skeletal system, and miscellaneous abnormalities such as nuchal thickening and ascites. Examples from our cohort included: presence of cerebral subependymal tubers and giant cell astrocytoma in association with cardiac rhabdomyomas in fetuses with tuberous sclerosis (Fig.16). Prenatal detection of a tumor in the region of foramen of Monro should raise the suspicion of congenital subependymal giant cell astrocytoma associated with tuberous sclerosis (Mirkin et al, 1999).

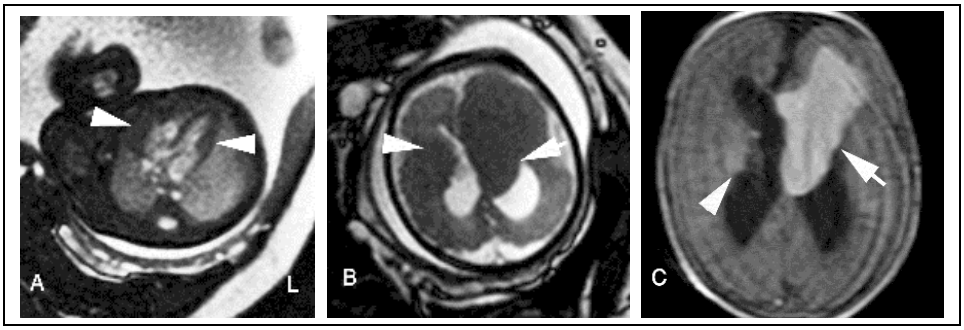

Fig. 16. Subependymal lesions in association with cardiac masses suggest the prenatal diagnosis of tuberous sclerosis. In-utero MRI using T2-SSFP at 29 weeks' gestation, of the chest (A) revealed multiple cardiac rhabdomyomas (arrowheads) associated with multiple cerebral subependymal masses (B) along the right lateral ventricle (arrowhead) as well as a large giant-cell astroytoma of the left foramen of Monro (arrow). Postnatal axial post-contrast MRI of the brain of the same case at the age of 7 days (C) documents enhancing congenital subependymal astrocytoma of foramen of Monro (arrow) as well as the non-enhancing subependymal tubers at the right lateral ventricle (arrowhead).

In our series, MRI documented the association of urinary tract dilatation with hypoplastic right heart in a fetus. These findings suggested the prenatal diagnosis of Kashani syndrome (Kashani et al, 1984). Identification of microcephaly, sacral agenesis in addition to Fallot's tetralogy, right sided aortic arch and aberrant left subclavian artery in another fetus suggested the prenatal diagnosis of cerebro-arthrodigital syndrome (Spranger et al, 1980) (Fig. 17).

In chromosomal abnormalities, fetal MRI identified Dandy Walker malformation in association with AV canal in a fetus with Trisomy 21 and holoprosencephaly in association with VSD (Fig.11A) in a fetus with trisomy 13.

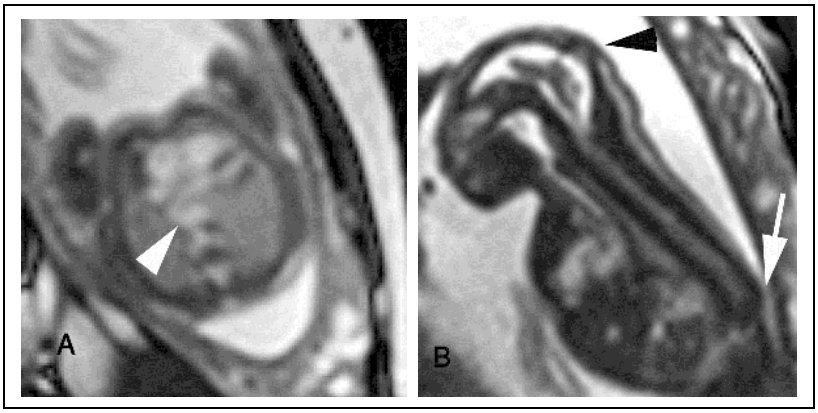

Fig. 17. Fetal MRI of a cerebro-arthrodigital syndrome at 20 weeks' gestation. (A) Axial T2-SSFP of heart shows right sided aortic arch with aberrant left subclavian artery (arrowhead) in association with Fallot's tetralogy. Sagittal MRI of the fetal body of the same fetus shows associated microcephaly (arrowhead) and sacral agenesis (arrow).

Fetal MRI documented prenatal ultrasonographic findings of AV canal defect, cerebral ventriculomegaly, and micromelia in a fetus with Fryns and Moerman syndrome (Fryns & Moerman, 1993). According to a report of 32 fetuses assessed for congenital heart disease, fetal MRI permitted identification of extracardiac anomalies associated with cardiac abnormalities. The authors document that MRI detected adjunctive fetal anomalies (particularly in CNS and neck) that US did not depict (Manganaro et al, 2008).

2.5 Fetal CMR limitations and future

Quantitative analysis of CMR was feasible in two fetuses with cardiac malformations by Fogel and colleagues. They found that measurements of ventricular volume could be obtained with MRI but not with fetal echocardiography. Both fetuses, however, were at advanced ages of gestation (34.5 and 36 weeks), and fetal sedation was necessary in one case. (Fogel et al, 2005).

Although cine MRI with the SSFP sequence is an established method of evaluation of cardiac function, imaging of a beating heart in a moving fetus is more complicated. The normal fetal heart rate of 120–160 beats per minute and unpredictable fetal body motion impair image quality owing to motion artifacts during MRI acquisition in utero (Guo et al, 2006). However, with the advent of parallel MRI technique, acquisition time is markedly reduced, yet image quality meets clinical requirements. Studies have shown that cine MRI in utero with steady-state acquisition and parallel imaging may be useful in the assessment of fetal body and cardiac movements. (Guo et al, 2006).Cine MR sequences for the evaluation of the contractile function of the fetal heart was attempted recently in fetuses with congenital heart diseases, yet it did not provide real-time images due to the high fetal heart rate and lack of fetal cardiac triggering (Manganaro et al, 2008).

Future fetal MRI sequences can take advantage of the improvement in radiofrequency and computing technology to decrease acquisition time and increase signal-to-noise ratio and image resolution. Fetal cardiac gating was attempted in sheep (Yamamura et al, 2010). As MRI technology advances, images of the heart are expected to be much clearer and to be acquired in a shorter time, allowing dramatic improvement in anatomic and functional MRI of the fetal heart. Reliable cardiac imaging in utero may have implications in the management of congenital heart disease, opening the possibility of fetal surgery (Saleem, 2008).

3. Conclusion

Fetal CMR facilitates visualization of the cardiac structures in multiple fetal body planes as well as cardiac axes. Fetal MR image analysis is possible using the anatomic segmental approach to congenital heart diseases. These features are potentially helpful for further characterization of cardiovascular abnormalities in utero. This chapter discusses the potentials of CMR in demonstrating normal and abnormal fetal heart rather than comparing it to echocardiography. Further studies are needed to evaluate the diagnostic utility and accuracy of in utero MRI of normal and abnormal hearts in correlation with the reference standard technique, fetal echocardiography. Further work is needed to advance MR imaging of the fetal heart through improvement of the available MRI sequences as well as introduction of functional MRI sequences and fetal cardiac gating.

4. Acknowledgment

I acknowledge Miss Amal Mahmoud, MRI operator at Cairo University, Egypt.

5. References

Brugger, PC.; Stuhr, F.; Linder, C.; Prayer, D. (2006). Methods of fetal MR: beyond T2-weighted imaging. *Eur J Radiol* Vol.57, pp. 172-181, 0720-048X

Carvalho, JS.; Mavrides, E; Shinebourne, EA; Campbell, S; Thilaganathan, B. (2002). Improving the effectiveness of routine prenatal screening for major congenital heart defects. *Heart* Vol.88, pp. 387-391, 1355-6037

Carvalho, JS.; Ho, SY.; Shinebourne, EA. (2005). Sequential segmental analysis in complex fetal cardiac abnormalities: a logical approach to diagnosis. *Ultrasound Obstet Gynecol* Vol.26 pp. 105–111, 0960-7692

Chung, HW.; Chen, CY.; Zimmerman, RA.; Lee, KW.; Lee, CC.; Chin, SC. (2000). T2-weighted Fast MR imaging with true FISP versus HASTE comparative efficacy in the evaluation of normal fetal brain maturation. Am J Roentgenol Vol.275, pp. 1375-1480, 0361-803X

Clements, H.; Duncan, KR.; Fielding K.; Gowland, PA.; Johnson, IR.; Baker, PB. (2000). Infants exposed to MRI in utero have a normal paediatric assessment at 9 months of age. *Br J Radiol* Vol.73, pp. 190-194, 0007-1285

Cohen, MS. (2001). Fetal diagnosis and management of congenital heart disease. *Clin Perinatol* Vol.28, pp. 11-29, 0095-5108

Finn, JP.; Nael, K.; Deshpande, V.; Ratib, O.; Laub, G. (2006). Cardiac MR imaging: state of the technology. *Radiology* Vol.241, No.2, pp. 338 – 354, 0033-8419

Fogel, MA.; Wilson, RD.; Flake, A.; Johnson, M.; Cohen, D.; McNeal, G.; Tian, ZY.; Rychik, J. (2005). Preliminary investigations into a new method of functional assessment of the fetal heart using a novel application of"real-time"cardiac magnetic resonance imaging. *Fetal Diagn Ther* Vol.20, pp. 475–480, 1015-3837

Forbus, GA.; Atz, AM.; Shirali, GS. (2004).Implications and limitations of an abnormal fetal echocardiogram. Am J Cardiol Vol.94, pp. 688-689, 0002-9149

Frates, M.; Kumar, A.; Benson, C.; Ward, V.; Tempany, C. (2004). Fetal anomalies: comparison of MR imaging and US for diagnosis. *Radiology* 2004; Vol.232, pp. 398-404, 0033-8419

Fryns, JP.; Moerman P. (1993). Short limbed dwarfism, genital hypoplasia, sparse hair, and vertebral anomalies: a variant of Ellis-van Creveld syndrome?. *J Med Genet* Vol.30, pp.322-324, 0022-2593

Fyler, DC.; Buckley, LP.; Hellenbrand, WE.; Cohn, HE. (1980). Report of the New England Regional Infant Care Program. *Pediatrics* Vol.65, Suppl. 375-461, 0031-4005

Glenn, OA.; Barkovich, AJ. (2006). Magnetic Resonance Imaging of the fetal brain and spine: an increasingly important tool in prenatal diagnosis, Part 1. *Am J Neuroradiol* Vol.27, pp. 1604-161, 0195-6108

Gorincour, G.; Bourliere-Najean, B.; BONELLO, b.; Philip, N.; Potier, A.; Kreitann, B.; Petit, P. (2007). Feasibility of fetal cardiac magnetic resonance imaging: preliminary experience. *Ultrasound Obstet Gynecol* Vol.29, pp. 105-108, 0960-7692

Guo, WY.; Ono, S.; Oi, S.; Shen, SH.; Wong, T.; Chung, HW.; Hung, JY. (2006). Dynamic motion analysis of fetuses with central nervous system disorders by cine magnetic resonance imaging using fast imaging employing steady state acquisition and parallel imaging. *J Neurosurg* Vol. 105, pp. 94 –100, 0022-3085

Hoffman, JI; Kaplan, S. (2002). The incidence of congenital heart disease. *J Am Coll Cardiol* Vol.39, pp. 1890-1900, 0735-1097

Kanal, E.; Borgstede, JP.; Barkovich, AJ.; Bell, C.; Bradley, WG.; Etheridge, S.; Felmlee, JP.; Froelich, JW.; Hayden, J.; Kaminski, EM.; Lester, JW Jr.; Scoumis, EA.; Zaremba

LA.; Zinniger, MD.; American College of Radiology. (2002). American College of Radiology white paper on MR safety. *Am J Roentgenol* Vol.178, pp. 1335-1347, 0361-803X

Kashani, IA.; Strom, CM.; Utley, JE.; Marin-Garcia, J.; Higgins, CB. (1984). Hypoplastic pulmonary arteries and aorta with obstructive uropathy in 2 siblings. Angiology Vol.35, No.4, pp. 252-256, 0003-3197

Kivelitz, DE.; Muhler, M.; Rake, A.; Scheer, I.; Chaoui, R. (2004). MRI of cardiac rhabdomyoma in the fetus. *Eur Radiol* Vol.14, No. 8, pp. 1513-1516, 0938-7994

Kleinman, CS.; Hobbin, JC.; Jaffe, CC.; Lynch, DC.; Tlaner, NS. (1980). Echocardiographic studies of the human fetus: prenatal diagnosis of congenital heart disease and cardiac dysrrhythmias. *Pediatrics* Vol.65, pp. 1059-1067, 0031-4005

Levine, D. (2006). Obstetric MRI. *Top Magn Reson Imaging* Vol.24, No.1, pp. 1-15, 0899-3459

Manganaro, L.; Savelli s.; Di Maurizio, M.; Perrone, A.; Tesei, J.; Francioso, A.; Angeletti, A.; Coratella, F.; Irimia, D.; Fierro, F.; Vnetriglia, F.; Ballesio, L. (2008). Potential role of fetal cardiac evaluation with magnetic resoance imaging: preliminary experience. *Prenat Diagn* Vol.28, pp. 148-156, 0197-3851

Manganaro, L.; Savelli s.; Di Maurizio, M.; et al. (2009). Assessment of congenital heart disease (CHD): Is there a role for fetal magnetic resonance imaging (MRI)?*European Journal of Radiology Vol.*72, pp. 172-180, 0720-048X

Mirkin, LD.; Ey, EH.; Chaparro, M. (1999). Congenital subependymal giant-cell astrocytoma: case report with prental ultrasonogram. *Pediatr Radiol* Vol. 29, No. 10, pp. 776-780, 0301-0449

O'Neill, JA.; Holcomb, GWIII.; Schnauffer, L.; Templeton, JM Jr.; Bishop, HC.; Ross, AJ III.; Duckett, JW.; Norwood, WI.; Ziegler, MM.; Koop, CE. (1988). Surgical experience with thirteen conjoined twins. *Ann Surg* Vol. 208, pp. 299-312, 0003-4932

Prakash, A.; Powell, A J.; Geva, T. (2010). Multimodality Noninvasive Imaging for Assessment of Congenital Heart Disease. *Circ Cardiovasc Imaging* Vol.3, No.1, pp. 112–125, 1941-9651

Saleem, SN. (2008). Feasibility of Magnetic resonance imaging (MRI) of the fetal heart using balanced Steady-State-Free-Precession (SSFP) sequence along fetal body and cardiac planes. *AJR* Vol. 191, pp. 1208-1215, 0361-803X

Saleem, SN.; Said, A-H.; Abdel-Raouf, M.; El-Kattan, EA.; Zaki, MS.; Madkour, N.; Mostafa, S. (2009). Fetal MRI in the evaluation of fetuses referred for sonographically suspected neural tube defects (NTDs): impact on diagnosis and management decision. *Neuroradiology* 2009 Vol.51, No.11, pp. 761-772, 0028-3940

Smith, RS.; Comstock, CH.; Kirk, JS.; Lee, W. (1995). Ultrasonographic left axis deviation: a marker for fetal anomalies. *Obstet Gynecol* Vol. 85, pp. 187-191, 0029-7844

Spranger, JW.; Schinzel, A.; Myers, T.; Ryan, J.; Giedion , A.; Opitz, JM. (1980). Cerebroarthrodigital syndrome: a newly recognized formal genesis syndrome in three patients with apparent arthromyodysplasia and sacral agenesis, brain malformation and digital hypoplasia. *Am J Med Genet* Vol.5, No. 2, pp. 13-24, 1552-4825

Tennstedt, C.; Chaoui, R.; Korner, H.; Dietel, M. (1999). Spectrum of congenital heart defects and extracardiac malformations associated with chromosomal abnormalities: results of a seven year necropsy study. *Heart* Vol.82, pp. 34-39, 1355-6037

Yamamura, J.; Frisch, M.; Ecker, H.; Graessner, J.; Hecher, K.; Adam, G.; Wedegärtner, U. (2010). Self-gating MR imaging of the fetal heart: comparison with real cardiac triggering. *European Radiology* Vol.21, No.1, pp., 142-149, 0938-7994

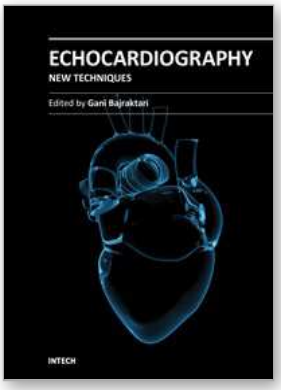

Echocardiography - New Techniques

Edited by Prof. Gani Bajraktari

ISBN 978-953-307-762-8
Hard cover, 218 pages
Publisher InTech
Published online 18, January, 2012
Published in print edition January, 2012

The book "Echocardiography - New Techniques" brings worldwide contributions from highly acclaimed clinical and imaging science investigators, and representatives from academic medical centers. Each chapter is designed and written to be accessible to those with a basic knowledge of echocardiography. Additionally, the chapters are meant to be stimulating and educational to the experts and investigators in the field of echocardiography. This book is aimed primarily at cardiology fellows on their basic echocardiography rotation, fellows in general internal medicine, radiology and emergency medicine, and experts in the arena of echocardiography. Over the last few decades, the rate of technological advancements has developed dramatically, resulting in new techniques and improved echocardiographic imaging. The authors of this book focused on presenting the most advanced techniques useful in today's research and in daily clinical practice. These advanced techniques are utilized in the detection of different cardiac pathologies in patients, in contributing to their clinical decision, as well as follow-up and outcome predictions. In addition to the advanced techniques covered, this book expounds upon several special pathologies with respect to the functions of echocardiography.

INTECH
open science | open minds

InTech Europe
University Campus STeP Ri
Slavka Krautzeka 83/A
51000 Rijeka, Croatia
Phone: +385 (51) 770 447
Fax: +385 (51) 686 166
www.intechopen.com

InTech China
Unit 405, Office Block, Hotel Equatorial Shanghai
No.65, Yan An Road (West), Shanghai, 200040, China
中国上海市延安西路65号上海国际贵都大饭店办公楼405单元
Phone: +86-21-62489820
Fax: +86-21-62489821